forests

MDPI

Article

Selective Restructuring of Soil Microbial Networks by *Tricholoma matsutake*: Spatial and Seasonal Predicted Microbial Shifts

Gi Beom Keum †, Eun-Kyung Bae †, Min-Jeong Kang, Min-Young Park, Na-Kyung Kang and Eung-Jun Park *

Department of Bioresources, National Institute of Forest Science, Suwon 16631, Republic of Korea; keumgb@gmail.com (G.B.K.); baeek@korea.kr (E.-K.B.); kangmj1020@korea.kr (M.-J.K.); min0young@naver.com (M.-Y.P.); hellonakyung@naver.com (N.-K.K.)

* Correspondence: pahkej@korea.kr; Tel.: +82-31-2901-1171

† These authors contributed equally to this work.

Abstract

The prized wild mushroom *Tricholoma matsutake* maintains distinctive microbiota within its dominant zone; however, the spatial and seasonal reorganization of microbiota from taxonomic and functional perspectives remain poorly understood. High-throughput amplicon sequencing was performed in warming (March–June) and cooling (September–December) seasons to compare microbial communities among *T. matsutake*-dominant (present, visible mycelium) and -nondominant soils (transition, adjacent with present; control, distant from fairy ring). Fungal and bacterial community structures in *T. matsutake*-dominant soils were obviously distinct (ANOSIM, R > 0.6, p = 0.001), and bacterial communities exhibited clear seasonal separation. The relative abundances of Ascomycota and Mortierellomycota significantly reduced, whereas mycorrhiza-helper bacteria, including *Paenibacillus*, *Bacillus*, and *Cohnella*, were enriched. Functional predictions suggested that the potential expression of cofactor and vitamin biosynthesis, nutrient degradation, and inorganic nutrient metabolism pathways may be enriched in *T. matsutake*-dominant soil. During the fruiting period, the expression of the predicted amino acid biosynthesis pathway may be reduced, whereas that of the cofactor/carrier/vitamin biosynthesis pathway may be enriched. Our findings suggest that *T. matsutake* dominance could be associated with the spatial and seasonal restructuring of soil microbial communities, potentially leading to the formation of functionally interconnected microbial networks. Therefore, this study predicts hidden ecological insights that, once biochemically validated, may be used to develop important strategies for the sustainable conservation and artificial cultivation of *T. matsutake*.

Keywords: microbiota; fungi-bacteria interactions; sustainable agriculture; amplicon sequencing

Check for updates

Academic Editor: Anna Zavarzina

Received: 5 March 2026
Revised: 9 April 2026
Accepted: 20 April 2026
Published: 22 April 2026

Copyright: © 2026 by the authors. Licensee MDPI, Basel, Switzerland. This article is an open access article distributed under the terms and conditions of the Creative Commons Attribution (CC BY) license.

1. Introduction

Natural forest soils harbor highly complex microbial communities that engage in diverse symbiotic interactions, contributing to nutrient cycling, host plant growth, and ecosystem functioning [1]. Within microbial communities, ectomycorrhizal fungi interact with their hosts and mediate carbon and nutrient exchange, thereby reshaping the surrounding soil environment and forming extensive interacting microbial communities [2,3]. *Tricholoma matsutake* (S. Ito & S. Imai) Singer—an ectomycorrhizal fungus with significant culinary value in Asia—is known to form symbiotic associations with members of Pinaceae

and Fagaceae depending on its geographic distribution [4,5]. In Korea and Japan, *Pinus densiflora* Siebold & Zucc. is identified as a major host plant forming symbiotic associations with *T. matsutake* [6]. *T. matsutake* develops characteristic mycelial aggregations known as fairy rings around *P. densiflora*, which are closely linked to fruiting body formation [2,7]. The fruiting bodies do not recur at a fixed location but expand outward by 10–20 cm annually, resulting in an outward-growing fairy ring [8]. However, soil eutrophication, deterioration of suitable habitat conditions, pest- and disease-driven mortality of *P. densiflora*, and forest fires have led to a rapid decline in the annual production of *T. matsutake* [9]. Therefore, it was listed as a vulnerable species on the IUCN Red List in 2019 [10].

Despite its declining natural yield, the demand for *T. matsutake* is exceptionally high, prompting ongoing efforts toward artificial cultivation, including spore application, inoculation with cultured mycelia, and transplantation of infected seedlings [11,12]. However, the ecological processes underpinning fairy ring formation in forest ecosystems are not driven solely by the mycelium of *T. matsutake*; they are also shaped by shifts in the soil environment mediated by surrounding microbial communities, including bacteria and fungi [13,14]. The soil in the fairy rings of *T. matsutake* is dominated by bacteria that utilize carbohydrates or amino acids exuded from the mycelium as energy sources. These bacteria promote mycelial development or influence interactions among microorganisms, thereby affecting mycelial growth [13]. Studies investigating the physicochemical properties of fairy ring versus non-fairy ring soils have provided valuable insights into the spatial characteristics of *T. matsutake* habitats and proposed strategic directions for enhancing their productivity [15,16].

In Korea, fruiting bodies of *T. matsutake* occur only during a limited autumn period (early September to early November), when both sufficient summer precipitation and cool environmental conditions, with soil temperatures of approximately <19 °C, are present [8,17,18]. In edible mushrooms other than *T. matsutake*, transition from the mycelium stage to fruiting body formation stage entails significant changes in soil- and substrate-associated microbial communities [19,20]. These findings suggest that *T. matsutake* may experience dynamic changes in microbial community composition within fairy rings in response to seasonal variations in mycelial activity and fruiting body development. Nonetheless, the possible effects of seasonal variations in bacterial and fungal communities in fairy ring and non-fairy ring soils are poorly understood, and spatial comparisons alone are insufficient to elucidate the ecological processes governing *T. matsutake* fruiting. Furthermore, previous studies have largely focused on taxonomic differences associated with spatial variation between fairy ring and non-fairy ring soils [14,21,22]. These studies have provided valuable insights into the characteristics of habitats dominated by *T. matsutake*; however, they have not fully addressed seasonal dynamics. Moreover, studies that simultaneously investigate the restructuring of microbial communities across both spatial and seasonal gradients, and explore whether these changes are associated with shifts in predicted functional potential, remain scarce. Consequently, incorporating the analysis of environmental shifts linked to seasonal dynamics as putative drivers of microbial communities is essential for understanding the ecological plasticity of the ectomycorrhizal system of *T. matsutake.* This approach can help identify microorganisms that are consistently associated with the nutritional and metabolic support required during the life cycle of *T. matsutake* from mycelial growth to fruiting body formation, providing a rational basis for the targeted selection and application of beneficial microbes, thereby promoting mycelial development and fruiting [20,23]. Additional experimental validation based on controlled bioassays, including biochemical and physiological analyses, can help clarify functionally important interactions that are activated and enable the identification of microorganisms that support critical periods of ecological activity. Such analyses may reveal the functional roles of

seasonally fluctuating *T. matsutake*-associated microbiota and enable the identification and application of beneficial microorganisms that support mycelial development and fruiting in *T. matsutake*.

In this study, we used high-throughput amplicon sequencing to investigate how spatial and seasonal variation in *T. matsutake* mycelial activity is putatively associated with the structural and functional reorganization of soil microbial communities while identifying microbial taxa that may be involved in these processes. We hypothesized that spatial and seasonal variation in *T. matsutake* activity would be associated with distinct shifts in microbial community structure and predicted functional profiles. Specifically, we expected that soils dominated by *T. matsutake* mycelium would exhibit enrichment of specific bacterial taxa potentially associated with mycorrhizal interactions, and that these patterns would further vary across seasons in relation to changes in mycelial activity and fruiting dynamics.

2. Materials and Methods

2.1. Sampling Information

The sampling site was a mountainous area in Hongcheon-gun, Gangwon-do, South Korea (37°44′25.90″ N, 127°38′53.5″ E), located between 307 and 392 m in elevation and dominated by *P. densiflora* in the forest canopy. During the sampling period, the mean temperatures were 6.1 °C in March and −5.5 °C in December, with the highest monthly mean temperature of 25.5 °C occurring in July. The annual precipitation was 1707.7 mm. The main soil type is sandy clay loam, which is a nutrient-poor soil with a pH of 3.7–5.1. Sampling was conducted at four seasonal time points (March, June, September, and December) in 2022. In this study, soils were classified into the following three zones based on the dominance of *T. matsutake*: present (PS), transition (TS), and control (CS) (Figure 1). PS was defined as the area where actively growing grayish-white mycelia of *T. matsutake* were visibly observed in the soil. The TS zone represented an area that had not yet been colonized by *T. matsutake* but was expected to be colonized later, according to the direction of mycelial expansion, because fairy rings typically expand outward by approximately 10–20 cm per year [7]. The CS zone was located >3 m away from the fairy ring and showed no evidence of *T. matsutake* colonization. The TS zone was separated from the PS zone by ~17 cm. Soil samples from each zone were collected after removing the litter layer at a depth of ~10 cm. Replicate samples for high-throughput amplicon sequencing were collected from three spatially distinct locations within a single fairy ring, each confirmed to contain *T. matsutake* mycelium. Sampling was limited to two locations for CS in September and for all zones in December (2 replicates). A total of 32 soil samples were homogenized and stored at −20 °C for eDNA extraction. To explore the relationship between soil environmental factors and *T. matsutake* colonization, soil physical properties (sand, silt, and clay) and chemical characteristics, including pH, organic matter content, total nitrogen, available phosphorus, electrical conductivity, exchangeable K^+, Ca^{2+}, Mg^{2+}, Na^+, water-soluble Fe, Mn, Zn, and inorganic nitrogen (NH_4^+-N and NO_3^--N), were analyzed. Soil samples collected in March (n = 3; PS = 2 and TS = 1), June (n = 3), and September (n = 3) were air-dried and sieved through a 2 mm mesh before detailed analysis.

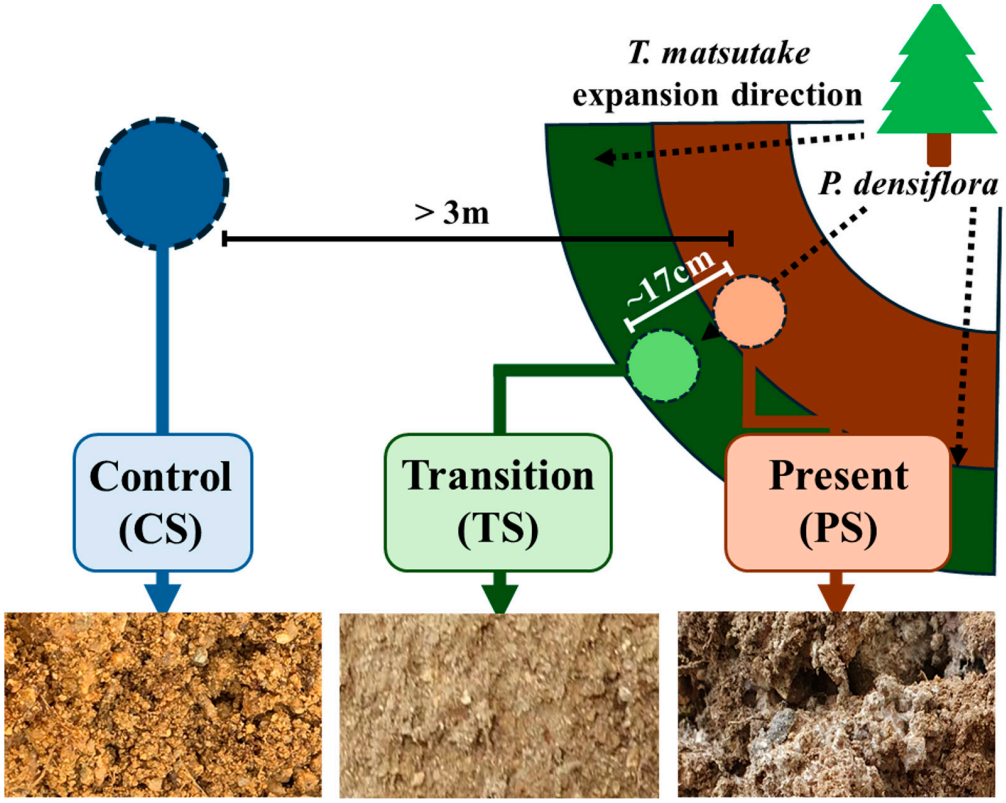


Figure 1. Soil sampling scheme across spatial zones of the *T. matsutake* fairy ring. "PS" represents locations within the fairy ring where active grayish-white mycelium was visually identified; "TS" represents the area predicted to be colonized along the direction of mycelial expansion; and "CS" represents sites located >3 m from the fairy ring with nondetectable *T. matsutake* colonization.

2.2. Sample Preprocessing & Sequencing

Environmental DNA was extracted from 500 mg of the soil sample using the DNeasy PowerSoil Kit (47016, Qiagen, Hilden, Germany), following the manufacturer's instructions. eDNA was quantified using VICTOR Nivo Multimode Microplate Reader (PerkinElmer, Waltham, MA, USA) with PicoGreen reagents. For amplicon-based microbial community analyses, the fungal 5.8S–ITS2 region and bacterial 16S rRNA V3–V4 region were amplified using PCR. Each PCR reaction contained 5× Herculase II Reaction Buffer, 1 mM dNTPs, 500 nM each of universal forward and reverse primers, 2.5 U of Herculase II Fusion DNA Polymerase (600675, Agilent Technologies, Santa Clara, CA, USA), and 5 ng of template eDNA. The primer sequences used were as follows: 5.8S–ITS2 (F: 5′-GCATCGATGAAGAACGCAGC-3′, R: 5′-TCCTCCGCTTATTGATATGC-3′) and 16S rRNA V3–V4 (F: 5′-CCTACGGGNGGCWGCAG-3′, R: 5′-GACTACHVGGGTATCTAATCC-3′). PCR cycling conditions were as follows: 95 °C for 3 min; 25 cycles of 95 °C for 30 s, 55 °C for 30 s, and 72 °C for 30 s; final extension at 72 °C for 5 min. Amplicons were purified using AMPure XP Beads (A63881, Agencourt Bioscience, Beverly, MA, USA). Sequencing libraries were prepared using the Nextera XT Index Kit (Illumina, San Diego, CA, USA). The final libraries were sequenced on an Illumina MiSeq platform (Illumina, San Diego, CA, USA) by Phyzen (Seongnam-si, Korea).

2.3. Bioinformatic Analysis Workflow

Raw ITS and 16S rRNA sequencing data were processed and analyzed using the Quantitative Insights into Microbial Ecology 2 platform version 2025.07 [24]. Adapters were removed from each read. Quality control, trimming, and removal of chimeric reads were performed using the DADA2 pipeline [25,26], and paired-end reads were merged

to generate amplicon sequence variants (ASVs). Multiple sequence alignment for phylogenetic diversity analyses was performed using Multiple Alignment using Fast Fourier Transform [27]. Taxonomic assignments for ASVs were conducted using a naïve Bayesian classifier trained on the UNITE + INSD ver10.0 database for fungi and the NCBI RefSeq 16S database for bacteria [28]. Alpha diversity was calculated with observed features, Chao1, Shannon, and Simpson indices [29–31]. Beta diversity of the fungal community was determined using Bray–Curtis and Jaccard distance metrics, as the high variability and alignment ambiguity of ITS regions limit reliable phylogenetic reconstruction across fungal taxa [32–34]. Beta diversity of bacterial communities was assessed based on weighted and unweighted UniFrac distance metrics and visualized using principal coordinate analysis plots [35]. Correlation networks among fungal and bacterial taxa were inferred using Sparse Estimation of Correlations among Microbiomes (SECOM) in MicrobiomeAnalyst 2.0 [36,37], with a correlation coefficient > |0.4| and $p < 0.05$. To enable the joint analysis of bacterial and fungal communities, relative abundance tables for each domain were independently normalized to a total sum of 1 and subsequently combined into a single dataset.

Functional prediction based on bacterial 16S rRNA gene amplicon sequences was conducted using Phylogenetic Investigation of Communities by Reconstruction of Unobserved States 2 (PICRUSt2) v 2.4.2 [38]. The Nearest Sequenced Taxon Index (NSTI), which quantifies the phylogenetic distance between 16S rRNA gene sequences and reference genomes used for functional prediction, was calculated to determine the accuracy of PICRUSt2 predictions. Functional annotations were assigned using the MetaCYC pathway database [39].

2.4. Statistical Analysis

The statistical significance of the soil physicochemical properties was determined using the Mann–Whitney test. Statistical significance of alpha diversity indices was evaluated using the Kruskal–Wallis H-test followed by Benjamini–Hochberg multiple comparison correction, implemented in GraphPad Prism version 8.00 (San Diego, CA, USA).

The relative abundance of microbial taxa and predicted functional genes was compared using the Statistical Analysis of Metagenomic Profiles software version 2.1.3 [40]. Differences in microbial taxa were assessed using Kruskal–Wallis H-test with Tukey–Kramer post hoc tests; differences in predicted functional pathways were evaluated using White's nonparametric *t*-test.

3. Results

3.1. Soil Physicochemical Properties

Physicochemical properties were analyzed for 9 soil samples (Supplementary Table S1). The average proportions of sand (PS, 60.5%; TS, 62.5%), silt (PS, 15.8%; TS, 13.9%), and clay (PS, 23.7%; TS, 23.6%) were comparable between PS and TS soils. When analyzed without considering seasonal variation, only exchangeable K^+ content was significantly higher in PS soil ($p < 0.05$, Supplementary Figure S1). Exchangeable Ca^{2+} and Mg^{2+} tended to be higher in PS soil than in TS soil in September (Supplementary Table S1).

3.2. Data Processing Results

Amplicon sequencing of the ITS2 (fungi) and 16S (bacteria) regions was performed using DNA extracted from mycosphere soil samples collected from *T. matsutake* habitats. Raw sequencing data were obtained from 32 samples (PS, $n = 11$; TS, $n = 11$; CS, $n = 10$) and have been deposited in the National Center for Biotechnology Information Sequence Read Archive (SRA) under the accession number PRJNA1337794. After completing preprocessing, including merging and removing chimeric reads, 2,591,220 high-quality fungal (average

80,976) and 1,429,526 bacterial (average 44,673) reads were obtained across the 32 samples (Supplementary Tables S2 and S3). Rarefaction curves indicated that the processed data possessed sufficient sequencing depth to characterize fungal and bacterial community profiles (Supplementary Figure S2). Across all samples, 3574 fungal and 13,021 bacterial ASVs were identified.

3.3. Fungal Microbial Diversity Analysis

Observed features and Chao1 indices did not differ significantly across all zones at any seasonal time point (Figure 2A). Although Shannon and Simpson indices showed significant differences among zones in March and September ($p < 0.05$), these patterns were not observed after correcting for false discovery rate ($q > 0.05$). Overall, the PS zone exhibited lower richness and evenness compared with the CS and TS zones across seasons. Principal coordinate analysis plots based on Bray–Curtis and Jaccard distances revealed a clear separation of the PS zone from the other zones, whereas the CS and TS zones showed largely similar fungal community structures (Figure 2B).

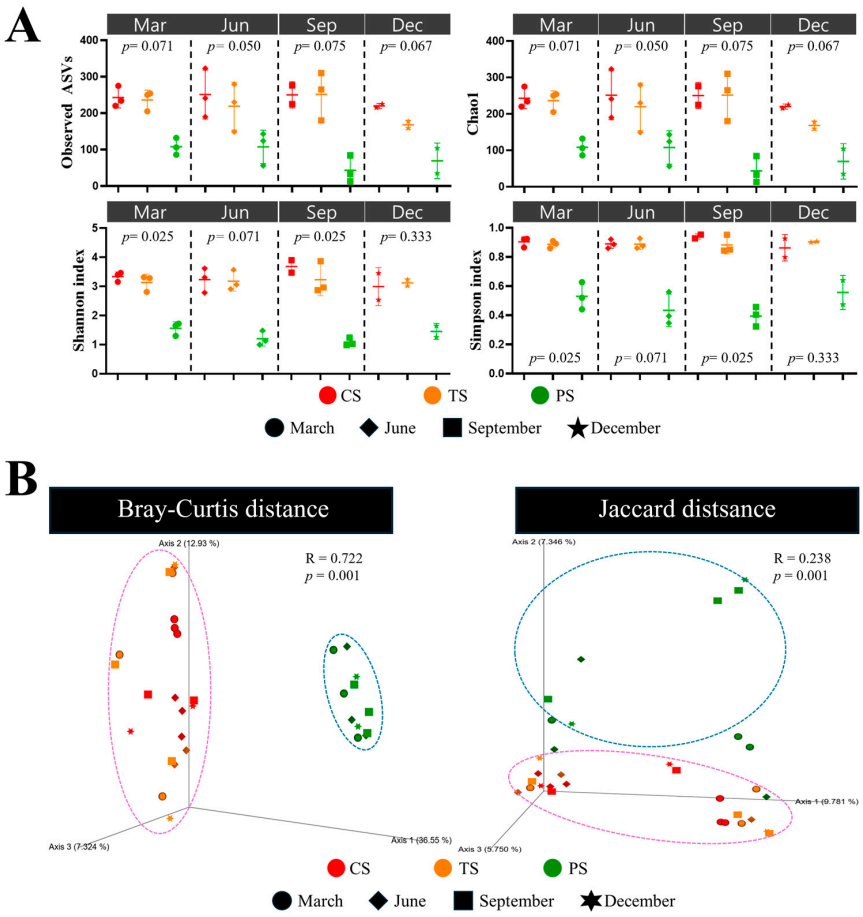


Figure 2. Microbial diversity of fungal communities in soil. (**A**) Separated scatter plots of fungal alpha diversity indices (observed features, Chao1, Shannon, and Simpson) in CS, TS, and PS soils across four seasonal sampling points. Each point represents an individual sample; lines with whiskers denote mean and standard deviation, reflecting the richness and evenness of fungal communities. (**B**) Principal coordinate analysis based on Bray–Curtis and Jaccard distance metrics shows differences in soil fungal community structures. Group dissimilarities were assessed using ANOSIM. R value indicates degree of intergroup separation; *p* value denotes statistical significance of community differences.

To assess fungal community patterns independent of the dominant influence of *T. matsutake*, we performed additional analyses excluding *T. matsutake* reads (Supplementary

Figure S3). The PS zone showed lower values of species richness than the CS and TS zones. By contrast, although evenness was lower than that in the other zones, it was relatively higher than that in the initial analysis. Fungal community structures continued to show distinct clustering of the PS zone, indicating that zone-level fungal community differences persisted even after removing *T. matsutake* sequences.

3.4. Bacterial Microbial Diversity Analysis

In March, the bacterial community showed significant zone-level differences in observed ASVs and Shannon index ($p < 0.05$); however, these patterns were nonsignificant after correcting for false discovery rate ($q > 0.05$) (Figure 3A). The bacterial diversity of the PS zone tended to decrease from March to December. Principal coordinate analysis plots based on beta diversity indicated a clear separation of the PS zone from the other zones, whereas the CS and TS zones exhibited similar bacterial community structures (Figure 3B). The PS zone showed a seasonal pattern in community structure, clustering into two groups corresponding to March–June and September–December.

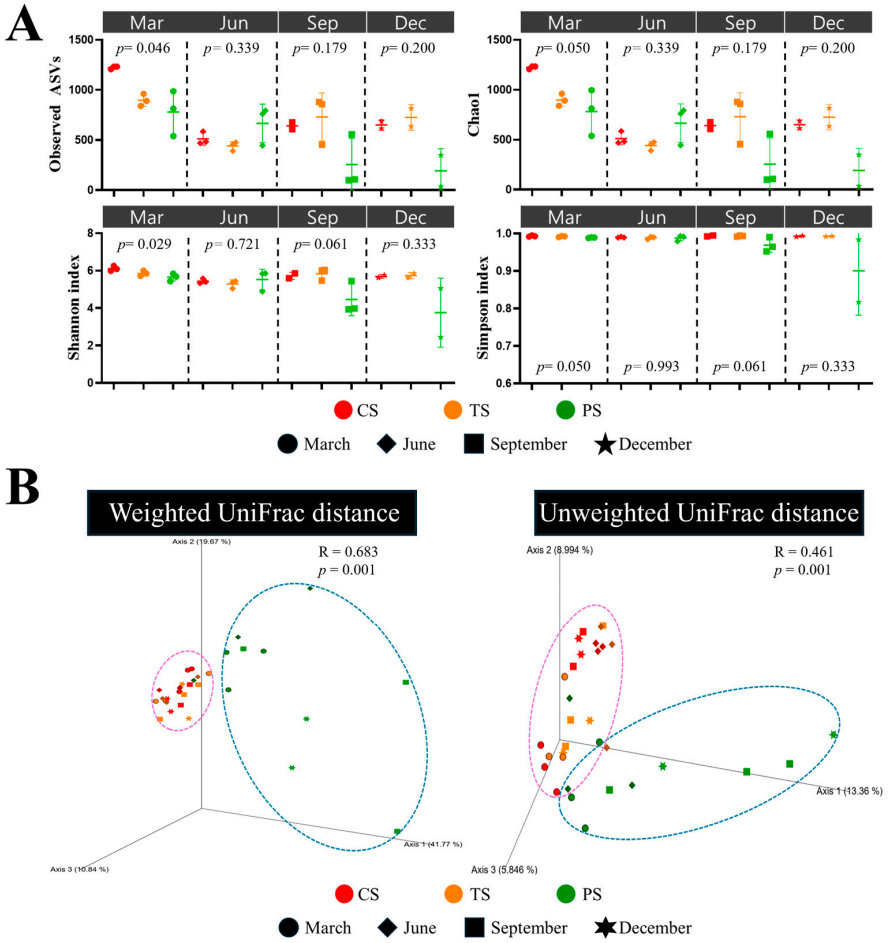


Figure 3. Microbial diversity of bacterial communities in soil. (**A**) Separated scatter plots of bacterial alpha diversity indices (observed features, Chao1, Shannon, and Simpson) in CS, TS, and PS soils across four seasonal sampling points. Each point represents an individual sample; lines with whiskers denote mean and standard deviation, reflecting the richness and evenness of bacterial communities. (**B**) Principal coordinate analysis based on weighted and unweighted UniFrac distance metrics show differences in soil bacterial community structures. Group dissimilarities were assessed using ANOSIM. R value indicates degree of intergroup separation; *p* value denotes statistical significance of community differences.

3.5. Fungal Microbial Composition

The taxonomic annotation of fungal communities across the three sampling zones revealed 14 phyla. The phyla Basidiomycota (38.37%–86.89%) and Mucoromycota (9.83%–28.88%) were dominant across all zones (Figure 4A). The phyla Ascomycota and Mortierellomycota were predominant in the CS (19.79%–31.31% and 2.25%–4.27%, respectively) and TS zones (16.68%–25.49% and 1.09%–7.74%, respectively) but showed markedly reduced abundance in the PS zone (2.04%–5.59% and 0.02%–0.56%, respectively).

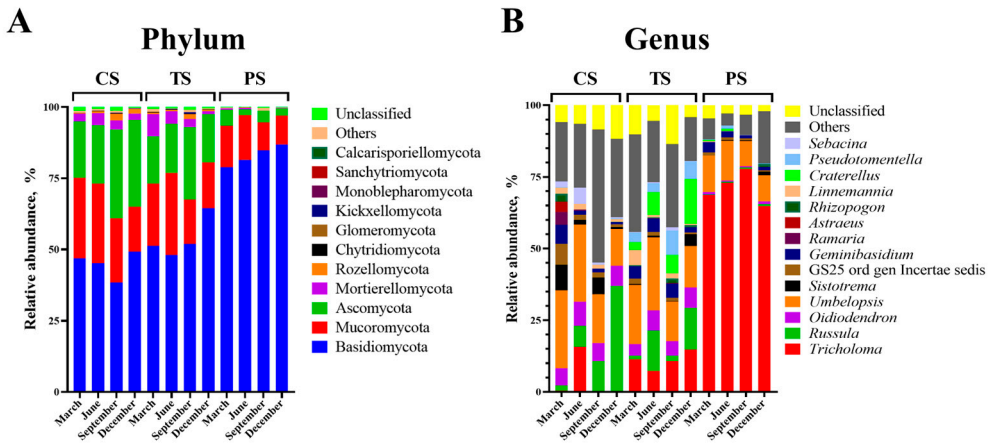


Figure 4. Microbial composition of fungi at the (**A**) phylum and (**B**) genus levels in CS, TS, and PS soils at each seasonal time point.

At the genus level, we identified 492 clades. The PS zone was strongly dominated by *Tricholoma* (64.83%–77.80%), which also appeared at notable levels in the TS zone (7.30%–14.83%) (Figure 4B). Within the PS zone, *T. matsutake* accounted for 64.71%–77.64% of the total fungal community, indicating that most *Tricholoma* sequences corresponded to *T. matsutake* (Figure 4, Supplementary Figure S4). By contrast, *T. matsutake* represented only 0.01%–0.14% of the fungal community in the TS zone, where *Tricholoma* was composed primarily of other species. Other dominant fungal genera included *Russula*, *Oidiodendron*, and *Umbelopsis*.

To elucidate fungal taxa associated with *T. matsutake* beyond its own dominance, fungal community composition was reevaluated after excluding *T. matsutake* reads (Supplementary Figure S4). In the PS zone, *Umbelopsis* became the most prominent genus within the remaining community. Conversely, *Russula* and *Oidiodendron* contributed minimally in the PS zone compared with the CS and TS zones. In the TS zone, *Craterellus* and *Pseudotomentella* were jointly dominant.

3.6. Bacterial Microbial Composition

In total, 24 bacterial phyla were identified across the three soil zones. Pseudomonadota (27.13%–42.29%) and Actinomycetota (10.57%–19.33%) were dominant across all zones; Bacillota was markedly enriched in the PS zone compared with the CS and TS zones (Figure 5A). Acidobacteria and Verrucomicrobiota were substantially reduced in the PS zone during September and December compared with March and June; Pseudomonadota and Bacteroidota showed increased abundance during these periods.

At the genus level, 399 clades were identified, with *Bradyrhizobium*, *Chthoniobacter*, and *Dictyobacter* representing major genera in the bacterial communities (Figure 5B). *Paenibacillus* showed notably higher relative abundance in the PS zone than in the other zones. In contrast to the patterns observed in other zones and during March and June, the PS zone exhibited a pronounced increase in *Usitatibacter*, *Staphylococcus*, and *Sphingorhabdus* in September and

December, leading to substantial shifts in community composition. *Bradyrhizobium* and *Terrimicrobium* showed a decreasing trend from March to December.

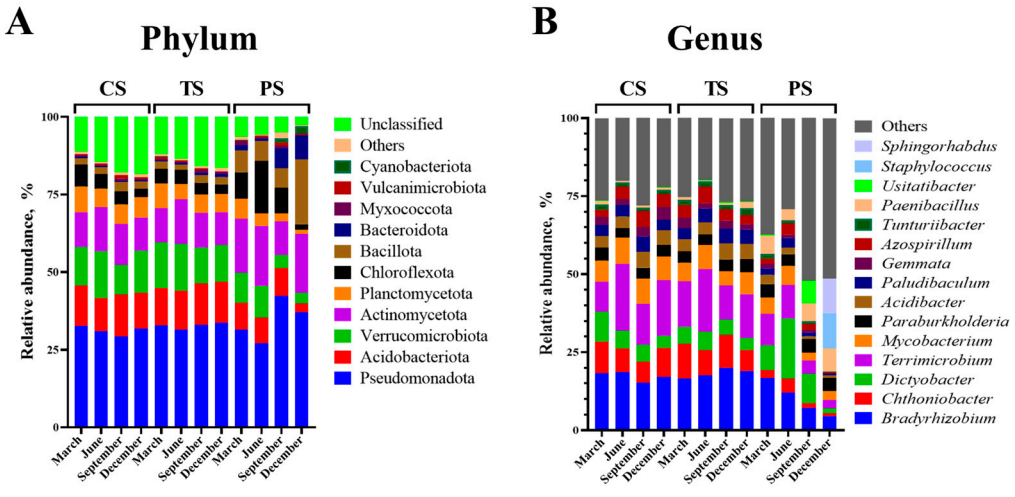


Figure 5. Microbial composition of bacteria at the (**A**) phylum and (**B**) genus levels in CS, TS, and PS soils at each seasonal time point.

Kruskal–Wallis H-test-based comparisons of relative abundance showed that *Actinomadura*, *Bacillus*, *Cohnella*, *Conexibacter*, *Paenibacillus*, and *Solirubrobacter* were significantly enriched in the PS zone compared with the TS and CS zones ($p < 0.05$) (Figure 6A). However, no significant seasonal differences were observed within the PS zone (Figure 6B). Consistent results were observed in the TS and CS zones (Supplementary Figure S5).

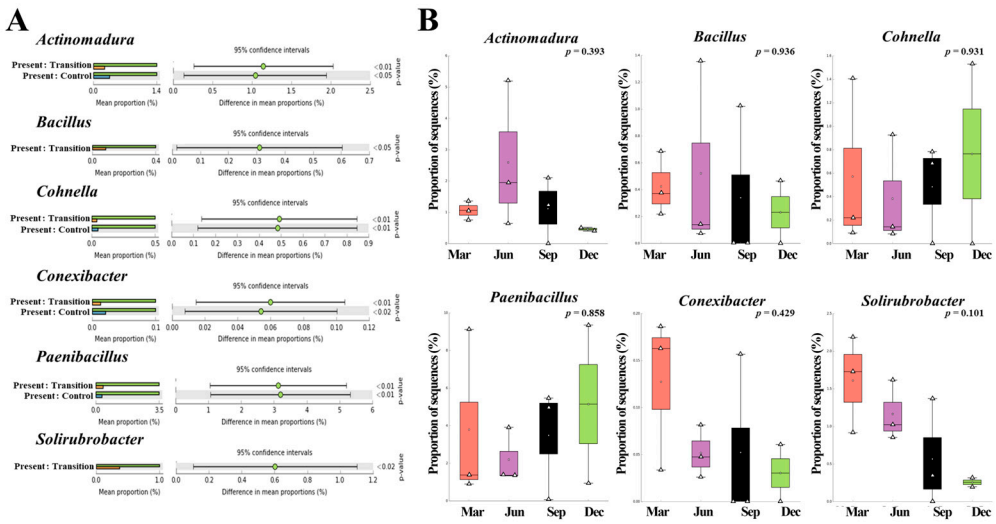


Figure 6. Differential abundance of genera in the bacterial microbiota among groups. (**A**) Post hoc extended error bar plots show significant differences among CS, TS, and PS soils. (**B**) Box plots show comparisons among the four seasonal time points in PS soils. Star indicates the mean, box represents the median and interquartile range (IQR: 25%–75% quartiles), and whiskers denote the minimum and maximum values within 1.5× the 25% and 75% quartiles.

3.7. Correlation of T. matsutake with Fungi and Bacteria

Normalized fungal and bacterial composition data were used to identify genus-level interactions with *T. matsutake* (Figure 7). For this analysis, *T. matsutake* was treated as an independent entity separate from *Tricholoma*, and correlations were evaluated using SECOM (Pearson2). This combined dataset represents a relative normalization model and does not reflect absolute abundance ratios between bacterial and fungal communities, which

would require qPCR-based 16S/ITS quantification. A total of 15 genera showed direct correlations with *T. matsutake*, of which only the bacterial genera *Aquicella* and *Cohnella* exhibited positive correlations. *Bacillus*, *Actinomadura*, and *Paenibacillus* exhibited positive correlations with *Cohnella*, indicating indirect positive associations with *T. matsutake*. The combined relative abundance of bacterial genera showing positive associations with *T. matsutake* through *Cohnella* and *Aquicella* represented 4.56% and 4.14% of the bacterial community in the CS and TS zones, respectively, whereas they reached 13.64% in the PS zone. *Solirubrobacter* and *Actinoallomurus* exhibited negative correlations with *Chthoniobacter* and *Paludibaculum*, respectively, suggesting additional indirect, positive associations with *T. matsutake*. By contrast, the bacterial genera *Paludibaculum* and *Chthoniobacter* and 11 fungal genera, including *Umbelopsis*, *Oidiodendron*, *Phialomyces*, and *Linnemannia*, showed negative correlations with *T. matsutake*. *Russula* positively correlated with *Linnemannia* and *Phialomyces*, suggesting an indirect negative association with *T. matsutake*.

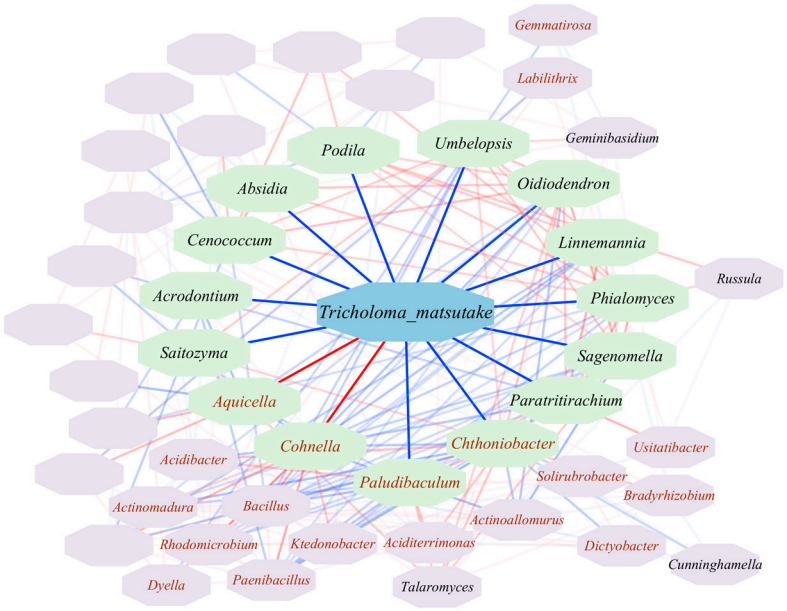


Figure 7. Co-occurrence patterns among *Tricholoma matsutake* and fungal and bacterial taxa were identified through network analysis. Nodes are colored differently according to their direct or indirect connections to *T. matsutake*. Black labels indicate fungi; brown labels indicate bacteria. Edges represent significant correlations ($p < 0.05$) with Sparse Estimation of Correlations among Microbiomes coefficients greater than |0.4|, where red and blue indicate positive and negative correlations, respectively.

3.8. Functional Predictions of Bacterial Communities

To compare the functional potential of bacterial communities across zones and seasons, metabolic functions were predicted using PICRUSt2. The NSTI values ranged from 0.100 to 0.342 across all soil samples, with mean values of CS 0.274, TS 0.273, and PS 0.228 (Supplementary Table S4), respectively, indicating that the quality of functional predictions was reasonably reliable [41]. Zone-level comparisons were performed between the TS and PS soils to identify functional shifts associated with *T. matsutake* dominance, whereas seasonal comparisons were conducted by grouping samples in the PS zone from March to June and September to December based on their similar community structures.

In total, 15 predicted metabolic pathways, including cofactor, carrier, and vitamin biosynthesis; amide, amidine, amine, and polyamine biosynthesis and degradation; amino acid degradation; inorganic nutrient metabolism; and the superpathway of chorismate metabolism, were significantly enriched in the PS zone compared with the TS zone (Sup-

plementary Figure S6A). By contrast, 9 predicted metabolic pathways, including amino acid biosynthesis, carbohydrate biosynthesis, and fatty acid and lipid biosynthesis, were significantly enriched in the TS zone.

Cofactor, carrier, or vitamin biosynthesis and the superpathway of chorismate metabolism were significantly enriched in PS zone from September to December compared with the PS zone from March to June; six pathways, including amino acid biosynthesis and aromatic compound degradation, were significantly enriched in the PS zone from March to June (Supplementary Figure S6B).

4. Discussion

Before the microbial community analysis, the soil physicochemical properties were examined, which showed that soil texture (sand, silt, and clay) was comparable between PS and TS soils. This suggests that chemical properties, rather than physical structure, may play a more vital role in shaping microbial community composition in *T. matsutake*-dominant soils. Remarkably, the significantly higher exchangeable K^+ content in PS soil suggests a potential association between potassium availability and *T. matsutake* dominance. Potassium plays essential roles in fungal metabolic processes and physiological functions, and previous studies have reported that potassium availability can affect microbial biomass, thereby supporting its potential importance in shaping microbial dynamics in this study [42–44]. Exchangeable Ca^{2+} and Mg^{2+} also tended to be higher in PS soil during September, corresponding to the fruiting period of *T. matsutake* in Korea. Calcium functions as a secondary messenger regulating fungal growth and development, and magnesium serves as a cofactor in enzymatic and metabolic processes, suggesting that these ions may contribute to favorable conditions for fruiting [45,46]. Moreover, previous studies have reported that K^+, Ca^{2+}, and Mg^{2+} are among the most abundant mineral elements accumulated in *T. matsutake* fruiting bodies [47]. Although the direct role of these cations in linking soil chemical properties to *T. matsutake* growth and fruiting remains to be clarified, our results suggest that *T. matsutake* dominance is associated with functionally relevant shifts in soil chemical properties and microbial communities, thereby potentially contributing to its growth and fruiting.

As reported in previous studies, fungal community diversity tended to be lower in the PS zone than in the CS and TS zones [21]. Even after excluding ASVs assigned to *T. matsutake*, the richness in the PS zone was consistently lower, suggesting that *T. matsutake* may suppress other fungal taxa that compete for ecological niches. Although the mechanisms of exclusion are unclear, as an ectomycorrhizal (ECM) fungus, it may directly or indirectly exclude competitors through spatial competition, alteration of soil physicochemical properties, or secretion of antifungal compounds [14,48,49]. The bacterial community in the PS zone appeared to exhibit a seasonal trend characterized by a progressive decline in species diversity from March to December (Figure 3A). A similar seasonal pattern has been reported by Zhelezova et al. [50], who reported increased bacterial abundance and diversity in spring following the resumption of microbial metabolism after winter. The relatively high diversity in March may reflect enhanced bacterial activity driven by increased soil moisture and decomposition of plant litter accumulated during winter [51]. Findings that soils dominated by *T. matsutake* exhibit reduced fungal and bacterial diversity in addition to the enrichment of specific taxa support the view that seasonal environmental fluctuations and presence of *T. matsutake* are associated with shifts in the structure and dynamics of bacterial communities [13].

Based on the microbial community composition analyses presented in Figures 4–6, *T. matsutake* putatively exerted strong selective influences on both fungal and bacterial communities. Consistent with studies reporting that the biomass of *T. matsutake* mycelia

suppresses the proliferation of coexisting fungal taxa [13,14], the PS zone showed marked abundance reduction in Ascomycota and Mortierellomycota. Most ECM genera commonly dominant in forest soils, including *Russula*, were scarce in the PS zone, whereas saprotrophic *Umbelopsis* were more abundant, consistent with previous reports [52–54]. This pattern may reflect the ability of *Umbelopsis* to either facilitate the growth of *T. matsutake* or tolerate the selective pressures imposed by *T. matsutake* [55]. By contrast, the TS zone was characterized by the dominance of ECM genera, such as *Craterellus* and *Pseudotomentella*, exhibiting a fungal community structure that appears to be less influenced by the effects observed in the PS zone. The TS and CS zones were not dominated by *T. matsutake*; however, the TS zone consistently showed dominance of the genus *Tricholoma* across all sampling periods. This pattern may indicate the potential for future fairy ring expansion and is supported by previous studies demonstrating that *T. matsutake* dominance progresses outward from the inner to the outer zones of the fairy ring [56].

The bacterial community in the PS zone was distinct from bacterial communities in the CS and TS zones and was characterized by the pronounced enrichment of Bacillota-belonging genera, including *Paenibacillus*, *Bacillus*, and *Cohnella*. Although these genera can be differentiated based on their metabolic products and cellular composition, they are recognized as mycorrhiza-helper bacteria or plant growth-promoting rhizobacteria that support ectomycorrhizal development through phosphate solubilization, siderophore production, and antimicrobial activity, and share similar sources of isolation and functional traits [57–66]. Additionally, *Actinomadura* and *Solirubrobacter*, which are involved in the decomposition of organic matter associated with carbon and nitrogen cycling, may indirectly contribute to the maintenance of a favorable habitat for *T. matsutake* [67–69]. Correlation network analysis exhibits direct and indirect positive correlations with a diverse range of genera (Figure 7). The positive correlation observed not only with the prominently enriched Bacillota-belonging genera but also with *Actinoallomurus*, which produces antibacterial and antifungal compounds [70], which may suggest that the presence of microbial taxa co-occurring with *T. matsutake* may contribute to the formation of selective microbial niches, within which complex networks of direct and indirect microbial interactions develop.

Supplementary Figure S6 shows pronounced contrasts in predicted functional profiles among the zones. Predicted biosynthetic pathways were enriched in the TS zone, whereas the PS zone showed increased predicted potential for nutrient degradation, inorganic nutrient metabolism, polyamine metabolism, and cofactor and vitamin biosynthesis. This pattern suggests that the *T. matsutake* mycosphere acts as an environmental filter associated with the enrichment of microbial taxa potentially related to nutrient transformation and recycling rather than biomass production [71,72]. The enrichment of predicted pathways related to nutrient cycling processes is consistent with genomic features reported for known mycorrhiza-helper bacteria (e.g., *Paenibacillus*, *Bacillus*, and *Cohnella*) [61,66,73–77]. Cofactor, carrier, and vitamin biosynthesis pathways, along with chorismate metabolism, were enriched in the PS zone, particularly during September–December, potentially indicating microbial processes associated with *T. matsutake* activity and nutrient dynamics [78,79]. PICRUSt2-based predictions represent inferred functional potential derived from 16S rRNA gene data and do not reflect actual gene expression, enzymatic activity, or metabolic flux. Therefore, these results require validation through biochemical or physiological assays. Such validation could include assays for siderophore production, phosphate solubilization, nitrogen fixation, and polyamine metabolism, as well as coculture or bioassay experiments, to determine their effects on *T. matsutake* growth. Moreover, amplicon-based eDNA approaches cannot distinguish between DNA derived from living and dead microorganisms, which may affect the interpretation of microbial community composition [80]. Despite these limitations, these results suggest that *T. matsutake* is associated with shifts in pre-

dicted microbial functional profiles and contributes to the formation of functional networks potentially favorable for its growth and fruiting.

5. Conclusions

Overall, this study provides an integrated space and seasonal perspective on the structural and functional reorganization of microbial communities within the fairy ring soils of *T. matsutake*. Our findings demonstrate that *T. matsutake* was associated with changes in microbial community composition and seasonal variation in functional pathways, including the enrichment of mycorrhiza-helper bacteria, such as *Paenibacillus*, *Bacillus*, and *Cohnella*, and metabolic processes potentially related to mycelial persistence and fruiting. These findings suggest that the ecological success of *T. matsutake* is associated with a selectively assembled microbial community, rather than being solely driven by fungal dominance, while highlighting the need for experimental validation of potentially beneficial taxa. Despite the limitations of amplicon-based analysis, this study provides a foundation for developing sustainable soil management and cultivation strategies for *T. matsutake*.

Supplementary Materials: The following supporting information can be downloaded at: https://www.mdpi.com/article/10.3390/f17050516/s1. Table S1. Soil physicochemical properties of PS and TS soil samples; Table S2. Raw data processing information of fungal samples; Table S3. Raw data processing information of bacterial samples; Table S4. PICRUSt2-based Weighted Nearest Sequenced Taxon Index (NSTI) data of soil samples; Figure S1. Comparison of soil physical and chemical properties between PS and TS zones of a *T. matsutake* fairy ring. (A) Soil texture composition (B) chemical properties; Figure S2. Rarefaction curves at various sequencing depths for ASVs of (A) fungal and (B) bacterial communities; Figure S3. (A) Alpha and (B) beta diversity analyses of soil fungal communities after excluding taxa classified as *Tricholoma matsutake*; Figure S4. (A) Phyla and (B) genera microbial composition of soil fungal communities after excluding taxa classified as *Tricholoma matsutake*; Figure S5. Box plots illustrate comparisons among the four seasonal time points in (A) TS and (B) CS soils. Star indicates the mean, box represents the median and interquartile range (IQR: 25%–75% quartiles), and whiskers denote the minimum and maximum values within 1.5× the 25% and 75% quartiles; Figure S6. PICRUSt2-predicted functional profiles of soil bacterial communities. (A) Extended error bar plot depicting MetaCyc functions that differ significantly between PS and TS soils. (B) Extended error bar plot depicting MetaCyc functions that differ significantly between the early (March–June) and late (September–December) seasonal periods in PS soils.

Author Contributions: Conceptualization, G.B.K. and E.-J.P.; Data curation, M.-J.K.; Formal analysis: G.B.K. and N.-K.K.; Funding acquisition: E.-K.B.; Investigation: M.-J.K., M.-Y.P. and E.-K.B.; Methodology: E.-K.B.; Project administration: E.-J.P.; Resources: G.B.K.; Software: G.B.K.; Supervision: E.-K.B. and E.-J.P.; Validation: E.-J.P.; Visualization: M.-Y.P. and N.-K.K.; Writing—original draft: G.B.K. and E.-K.B.; Writing—review and editing: E.-K.B. and E.-J.P. All authors have read and agreed to the published version of the manuscript.

Funding: This research was funded by the National Institute of Forest Science under grant (Forest Science Research project number FE0500-2026-01-2026) to E.-K.B.

Data Availability Statement: The datasets analyzed for this study can be found in the National Center for Biotechnology Information database under Sequence Read Archive (SRA) with accession number PRJNA1337794.

Acknowledgments: The authors are grateful for the support provided by the National Institute of Forest Science, Republic of Korea. The authors have reviewed and edited the output and take full responsibility for the content of this publication.

Conflicts of Interest: The authors declare no conflicts of interest. The funders had no role in the design of the study; in the collection, analyses, or interpretation of data. No ethical approval was required for this study as it did not involve human or animal subjects.

Abbreviations

The following abbreviations are used in this manuscript:

TM	*Tricholoma matsutake*
ASVs	Amplicon sequence variants
PICRUSt2	Phylogenetic Investigation of Communities by Reconstruction of Unobserved States 2

References

1. Chen, Q.; Song, Y.; An, Y.; Lu, Y.; Zhong, G. Soil Microorganisms: Their Role in Enhancing Crop Nutrition and Health. *Diversity* **2024**, *16*, 734. [CrossRef]
2. Lian, C.; Narimatsu, M.; Nara, K.; Hogetsu, T. Tricholoma matsutake in a natural Pinus densiflora forest: Correspondence between above-and below-ground genets, association with multiple host trees and alteration of existing ectomycorrhizal communities. *New Phytol.* **2006**, *171*, 825–836. [CrossRef] [PubMed]
3. Stuart, E.K.; Plett, K.L. Digging deeper: In search of the mechanisms of carbon and nitrogen exchange in ectomycorrhizal symbioses. *Front. Plant Sci.* **2020**, *10*, 1658. [CrossRef] [PubMed]
4. Endo, N.; Dokmai, P.; Suwannasai, N.; Phosri, C.; Horimai, Y.; Hirai, N.; Fukuda, M.; Yamada, A. Ectomycorrhization of Tricholoma matsutake with Abies veitchii and Tsuga diversifolia in the subalpine forests of Japan. *Mycoscience* **2015**, *56*, 402–412. [CrossRef]
5. Li, Q.; Xiong, C.; Li, X.; Jin, X.; Huang, W. Ectomycorrhization of Tricholoma matsutake with Quercus aquifolioides affects the endophytic microbial community of host plant. *J. Basic Microbiol.* **2018**, *58*, 238–246. [CrossRef]
6. Yun, W.; Hall, I.R.; Evans, L.A. Ectomycorrhizal fungi with edible fruiting bodies 1. Tricholoma matsutake and related fungi. *Econ. Bot.* **1997**, *51*, 311–327. [CrossRef]
7. Ogawa, M. Microbial ecology of mycorrhizal fungus—*Tricholoma matsutake* (Ito et Imai) Sing. in Pine Forest II. Mycorrhiza formed by Tricholoma matsutake. *Bull. Gov. For. Exp. Stn. Ringyo Shikenjo Kenkyu Hokoku* **1975**, *278*, 21–49.
8. Narimatsu, M.; Koiwa, T.; Masaki, T.; Sakamoto, Y.; Ohmori, H.; Tawaraya, K. Relationship between climate, expansion rate, and fruiting in fairy rings ('shiro') of an ectomycorrhizal fungus Tricholoma matsutake in a Pinus densiflora forest. *Fungal Ecol.* **2015**, *15*, 18–28. [CrossRef]
9. Furukawa, H.; Tokuoka, K.; Mizuno, A.; Katagiri, K.; Masuno, K.; Tanaka, Y.; Oya, S.; Yamada, A. Long-term effects of forest management on the dynamics of Tricholoma matsutake harvest over 41 years in a Pinus densiflora forest in Nagano Prefecture, Japan. *Mycoscience* **2024**, *65*, 298–306. [CrossRef]
10. Brandrud, T.-E. *Tricholoma matsutake (Errata Version Published in 2022). The IUCN Red List of Threatened Species*; IUCN: Gland, Switzerland, 2020; p. e.T76267712A223017164. [CrossRef]
11. Yamanaka, T.; Yamada, A.; Furukawa, H. Advances in the cultivation of the highly-prized ectomycorrhizal mushroom Tricholoma matsutake. *Mycoscience* **2020**, *61*, 49–57. [CrossRef]
12. Ka, K.-H.; Kim, H.-S.; Hur, T.; Park, H.; Jeon, S.; Ryoo, R.; Jang, Y. Analysis of environment and production of Tricholoma matsutake in matsutake-infected pine trees. *Korean J. Mycol.* **2018**, *46*, 34–42.
13. Oh, S.-Y.; Fong, J.J.; Park, M.S.; Lim, Y.W. Distinctive feature of microbial communities and bacterial functional profiles in Tricholoma matsutake dominant soil. *PLoS ONE* **2016**, *11*, e0168573. [CrossRef] [PubMed]
14. Zhou, J.; Gui, H.; Yang, S.; Yang, X.; Shi, L. Fungal Interactions Matter: Tricholoma matsutake Domination Affect Fungal Diversity and Function in Mountain Forest Soils. *Biology* **2021**, *10*, 1051. [CrossRef] [PubMed]
15. Oh, S.-Y.; Lim, Y.W. Root-associated bacteria influencing mycelial growth of Tricholoma matsutake (pine mushroom). *J. Microbiol.* **2018**, *56*, 399–407. [CrossRef] [PubMed]
16. Park, K.H.; Oh, S.-Y.; Yoo, S.; Park, M.S.; Fong, J.J.; Lim, Y.W. Successional Change of the Fungal Microbiome Pine Seedling Roots Inoculated With Tricholoma matsutake. *Front. Microbiol.* **2020**, *11*, 574146. [CrossRef]
17. Kurokochi, H.; Lian, C. Change in Soil Temperature and Moisture Content After Removal of the A0 Layer in *Pinus densiflora* Forest: A Case Study of a Mountain Where Matsutake Mushrooms (*Tricholoma matsutake*) Grow. *Curr. Trends For. Res.* **2018**, *2018*, CTFR-111.
18. Wang, Y.; Yu, F.; Zhang, C.; Li, S. Tricholoma matsutake: An edible mycorrhizal mushroom of high socioeconomic relevance in China. *Rev. Mex. Micol.* **2017**, *46*, 55–61.
19. Bánfi, R.; Pohner, Z.; Szabó, A.; Herczeg, G.; Kovács, G.M.; Nagy, A.; Márialigeti, K.; Vajna, B. Succession and potential role of bacterial communities during *Pleurotus ostreatus* production. *FEMS Microbiol. Ecol.* **2021**, *97*, fiab125. [CrossRef]
20. Zhang, C.; Shi, X.; Zhang, J.; Zhang, Y.; Wang, W. Dynamics of soil microbiome throughout the cultivation life cycle of morel (*Morchella sextelata*). *Front. Microbiol.* **2023**, *14*, 979835. [CrossRef]

21. Kim, M.; Yoon, H.; You, Y.-H.; Kim, Y.-E.; Woo, J.-R.; Seo, Y.; Lee, G.-M.; Kim, Y.J.; Kong, W.-S.; Kim, J.-G. Metagenomic analysis of fungal communities inhabiting the fairy ring zone of *Tricholoma matsutake*. *J. Microbiol. Biotechnol.* **2013**, *23*, 1347–1356. [CrossRef]
22. An, G.-H.; Cho, J.-H.; Kim, O.-T.; Han, J.-G. Metagenomic Analysis of Bacterial and Fungal Communities Inhabiting Shiro Dominant Soils of Two Production Regions of Tricholoma Matsutake S. Ito & S. Imai in Korea. *Forests* **2021**, *12*, 758. [CrossRef]
23. Yue, Y.; Hao, H.; Wang, Q.; Xiao, T.; Zhang, Y.; Chen, Q.; Chen, H.; Zhang, J. Dynamics of the soil microbial community associated with Morchella cultivation: Diversity, assembly mechanism and yield prediction. *Front. Microbiol.* **2024**, *15*, 1345231. [CrossRef]
24. Bolyen, E.; Rideout, J.R.; Dillon, M.R.; Bokulich, N.A.; Abnet, C.C.; Al-Ghalith, G.A.; Alexander, H.; Alm, E.J.; Arumugam, M.; Asnicar, F.; et al. Reproducible, interactive, scalable and extensible microbiome data science using QIIME 2. *Nat. Biotechnol.* **2019**, *37*, 852–857. [CrossRef] [PubMed]
25. Rosen, M.J.; Callahan, B.J.; Fisher, D.S.; Holmes, S.P. Denoising PCR-amplified metagenome data. *BMC Bioinform.* **2012**, *13*, 283. [CrossRef] [PubMed]
26. Callahan, B.J.; McMurdie, P.J.; Rosen, M.J.; Han, A.W.; Johnson, A.J.A.; Holmes, S.P. DADA2: High-resolution sample inference from Illumina amplicon data. *Nat. Methods* **2016**, *13*, 581–583. [CrossRef]
27. Katoh, K.; Standley, D.M. MAFFT Multiple Sequence Alignment Software Version 7: Improvements in Performance and Usability. *Mol. Biol. Evol.* **2013**, *30*, 772–780. [CrossRef]
28. Abarenkov, K.; Nilsson, R.H.; Larsson, K.-H.; Taylor, A.F.S.; May, T.W.; Frøslev, T.G.; Pawlowska, J.; Lindahl, B.; Põldmaa, K.; Truong, C.; et al. The UNITE database for molecular identification and taxonomic communication of fungi and other eukaryotes: Sequences, taxa and classifications reconsidered. *Nucleic Acids Res.* **2023**, *52*, D791–D797. [CrossRef]
29. Chao, A. Nonparametric estimation of the number of classes in a population. *Scand. J. Stat.* **1984**, *11*, 265–270.
30. Simpson, E.H. Measurement of diversity. *Nature* **1949**, *163*, 688. [CrossRef]
31. Shannon, C.E. A mathematical theory of communication. *Bell Syst. Tech. J.* **1948**, *27*, 379–423. [CrossRef]
32. Goodrich, J.K.; Di Rienzi, S.C.; Poole, A.C.; Koren, O.; Walters, W.A.; Caporaso, J.G.; Knight, R.; Ley, R.E. Conducting a microbiome study. *Cell* **2014**, *158*, 250–262. [CrossRef]
33. Bray, J.R.; Curtis, J.T. An Ordination of the Upland Forest Communities of Southern Wisconsin. *Ecol. Monogr.* **1957**, *27*, 325–349. [CrossRef]
34. Jaccard, P. Étude comparative de la distribution florale dans une portion des Alpes et des Jura. *Bull. Soc. Vaudoise Sci. Nat.* **1901**, *37*, 547–579.
35. Lozupone, C.; Knight, R. UniFrac: A New Phylogenetic Method for Comparing Microbial Communities. *Appl. Environ. Microb.* **2005**, *71*, 8228–8235. [CrossRef]
36. Lin, H.; Eggesbø, M.; Peddada, S.D. Linear and nonlinear correlation estimators unveil undescribed taxa interactions in microbiome data. *Nat. Commun.* **2022**, *13*, 4946. [CrossRef]
37. Lu, Y.; Zhou, G.; Ewald, J.; Pang, Z.; Shiri, T.; Xia, J. MicrobiomeAnalyst 2.0: Comprehensive statistical, functional and integrative analysis of microbiome data. *Nucleic Acids Res.* **2023**, *51*, W310–W318. [CrossRef]
38. Douglas, G.M.; Maffei, V.J.; Zaneveld, J.R.; Yurgel, S.N.; Brown, J.R.; Taylor, C.M.; Huttenhower, C.; Langille, M.G.I. PICRUSt2 for prediction of metagenome functions. *Nat. Biotechnol.* **2020**, *38*, 685–688. [CrossRef] [PubMed]
39. Caspi, R.; Billington, R.; Keseler, I.M.; Kothari, A.; Krummenacker, M.; Midford, P.E.; Ong, W.K.; Paley, S.; Subhraveti, P.; Karp, P.D. The MetaCyc database of metabolic pathways and enzymes—A 2019 update. *Nucleic Acids Res.* **2020**, *48*, D445–D453. [CrossRef] [PubMed]
40. Parks, D.; Beiko, R. STAMP: Statistical Analysis of Metagenomic Profiles. In *Encyclopedia of Metagenomics*; Nelson, K.E., Ed.; Springer: New York, NY, USA, 2013; pp. 1–6. [CrossRef]
41. Canarini, A.; Schmidt, H.; Fuchslueger, L.; Martin, V.; Herbold, C.W.; Zezula, D.; Gündler, P.; Hasibeder, R.; Jecmenica, M.; Bahn, M.; et al. Ecological memory of recurrent drought modifies soil processes via changes in soil microbial community. *Nat. Commun.* **2021**, *12*, 5308. [CrossRef] [PubMed]
42. Dominguez-Nuñez, J.A.; Benito, B.; Berrocal-Lobo, M.; Albanesi, A. Mycorrhizal Fungi: Role in the Solubilization of Potassium. In *Potassium Solubilizing Microorganisms for Sustainable Agriculture*; Meena, V.S., Maurya, B.R., Verma, J.P., Meena, R.S., Eds.; Springer: New Delhi, India, 2016; pp. 77–98. [CrossRef]
43. Yuan, L.; Huang, J.; Christie, P.; Li, X. Influence of Potassium Supply on Growth and Uptake of Nitrogen, Phosphorus, and Potassium by Three Ectomycorrhizal Fungal Isolates In Vitro. *J. Plant Nutr.* **2005**, *28*, 271–284. [CrossRef]
44. Chen, Z.; Zhang, K.; Su, F.; Wang, X.; Wang, Z. Potassium mediates succession of microbial community and nitrogen functions under long-term sloping cultivation with soybean. *Agric. Ecosyst. Environ.* **2025**, *382*, 109466. [CrossRef]
45. Rózsa, M.; Măniuțiu, D.-N.; Egyed, E. Influence of magnesium (Mg) source on the *Cordyceps militaris* (L.) mushroom mycelium growth. *Curr. Trends Nat. Sci.* **2021**, *10*, 333–340. [CrossRef]
46. Roy, A.; Kumar, A.; Baruah, D.; Tamuli, R. Calcium signaling is involved in diverse cellular processes in fungi. *Mycology* **2020**, *12*, 10–24. [CrossRef]

47. Li, T.; Zhang, J.; Shen, T.; Shi, Y.-D.; Yang, S.-B.; Zhang, T.; Li, J.-Q.; Wang, Y.-Z.; Liu, H.-G. Mineral element content in prized matsutake mushroom (*Tricholoma matsutake*) collected in China. *Chem. Pap.* **2013**, *67*, 672–676. [CrossRef]
48. Zotti, M.; Bonanomi, G.; Mazzoleni, S. Fungal fairy rings: History, ecology, dynamics and engineering functions. *IMA Fungus* **2025**, *16*, e138320. [CrossRef]
49. Nishino, K.; Shiro, M.; Okura, R.; Oizumi, K.; Fujita, T.; Sasamori, T.; Tokitoh, N.; Yamada, A.; Tanaka, C.; Yamaguchi, M.; et al. The (oxalato)aluminate complex as an antimicrobial substance protecting the "shiro" of *Tricholoma matsutake* from soil micro-organisms. *Biosci. Biotechnol. Biochem.* **2017**, *81*, 102–111. [CrossRef]
50. Zhelezova, A.; Chernov, T.; Nikitin, D.; Tkhakakhova, A.; Ksenofontova, N.; Zverev, A.; Kutovaya, O.; Semenov, M. Seasonal Dynamics of Soil Bacterial Community under Long-Term Abandoned Cropland in Boreal Climate. *Agronomy* **2022**, *12*, 519. [CrossRef]
51. Landesman, W.J.; Freedman, Z.B.; Nelson, D.M. Seasonal, sub-seasonal and diurnal variation of soil bacterial community composition in a temperate deciduous forest. *FEMS Microbiol. Ecol.* **2019**, *95*, fiz002. [CrossRef]
52. Wardle, D.A.; Lindahl, B.D. Disentangling global soil fungal diversity. *Science* **2014**, *346*, 1052–1053. [CrossRef]
53. Geml, J.; Laursen, G.A.; Herriott, I.C.; McFarland, J.M.; Booth, M.G.; Lennon, N.; Chad Nusbaum, H.; Lee Taylor, D. Phylogenetic and ecological analyses of soil and sporocarp DNA sequences reveal high diversity and strong habitat partitioning in the boreal ectomycorrhizal genus *Russula* (Russulales; Basidiomycota). *New Phytol.* **2010**, *187*, 494–507. [CrossRef] [PubMed]
54. Brinkmann, N.; Schneider, D.; Sahner, J.; Ballauff, J.; Edy, N.; Barus, H.; Irawan, B.; Budi, S.W.; Qaim, M.; Daniel, R.; et al. Intensive tropical land use massively shifts soil fungal communities. *Sci. Rep.* **2019**, *9*, 3403. [CrossRef]
55. Ogawa, M. Studies on the artificial reproduction of Tricholoma matsutake (S Ito et Imai) Sing. III. Effects of growth promotion of natural products on the vegetative growth of T. matsutake. *Trans. Mycol. Soc. Jpn.* **1976**, *17*, 492. (In Japanese)
56. Kang, N.-K.; Kang, M.-J.; Keum, G.-B.; An, C.; Park, E.-J.; Bae, E.-K. Soil Chemistry and Microbial Community Patterns Across Tricholoma matsutake Fairy-Ring Developmental Stages in Yeongju, South Korea. *Mycobiology* **2026**, *54*, 78–88. [CrossRef] [PubMed]
57. Frey-Klett, P.; Garbaye, J.; Tarkka, M. The mycorrhiza helper bacteria revisited. *New Phytol.* **2007**, *176*, 22–36. [CrossRef] [PubMed]
58. Barragán-Soriano, J.L.; Pérez-Moreno, J.; Almaraz-Suárez, J.J.; Carcaño-Montiel, M.G.; Medrano-Ortiz, K.I. Inoculation with an edible ectomycorrhizal fungus and bacteria increases growth and improves the physiological quality of Pinus montezumae Lamb. *Rev. Chapingo Ser. Cienc. For. Ambiente* **2018**, *24*, 3–16. [CrossRef]
59. Hildebrandt, U.; Ouziad, F.; Marner, F.-J.; Bothe, H. The bacterium Paenibacillus validus stimulates growth of the arbuscular mycorrhizal fungus *Glomus intraradices* up to the formation of fertile spores. *FEMS Microbiol. Lett.* **2006**, *254*, 258–267. [CrossRef] [PubMed]
60. Etesami, H.; Jeong, B.R.; Glick, B.R. Contribution of arbuscular mycorrhizal fungi, phosphate–solubilizing bacteria, and silicon to P uptake by plant. *Front. Plant Sci.* **2021**, *12*, 699618. [CrossRef]
61. Grady, E.N.; MacDonald, J.; Liu, L.; Richman, A.; Yuan, Z.-C. Current knowledge and perspectives of Paenibacillus: A review. *Microb. Cell Fact.* **2016**, *15*, 203. [CrossRef]
62. Kämpfer, P.; Rossello-Mora, R.; Falsen, E.; Busse, H.-J.; Tindall, B.J. *Cohnella thermotolerans* gen. nov., sp. nov., and classification of '*Paenibacillus hongkongensis*' as *Cohnella hongkongensis* sp. nov. *Int. J. Syst. Evol. Microbiol.* **2006**, *56*, 781–786. [CrossRef]
63. Kim, E.S.; Kim, B.-S.; Kim, K.-Y.; Woo, H.-M.; Lee, S.-M.; Um, Y. Aerobic and anaerobic cellulose utilization by Paenibacillus sp. CAA11 and enhancement of its cellulolytic ability by expressing a heterologous endoglucanase. *J. Biotechnol.* **2018**, *268*, 21–27. [CrossRef]
64. Shiratori, H.; Tagami, Y.; Beppu, T.; Ueda, K. Cohnella fontinalis sp. nov., a xylanolytic bacterium isolated from fresh water. *Int. J. Syst. Evol. Microbiol.* **2010**, *60*, 1344–1348. [CrossRef]
65. Teng, J.; Woo, P.; Leung, K.; Lau, S.; Wong, M.; Yuen, K. Pseudobacteraemia in a patient with neutropenic fever caused by a novel paenibacillus species: *Paenibacillus hongkongensis* sp. nov. *Mol. Pathol.* **2003**, *56*, 29. [CrossRef]
66. Wen, Y.; Wu, X.; Teng, Y.; Qian, C.; Zhan, Z.; Zhao, Y.; Li, O. Identification and analysis of the gene cluster involved in biosynthesis of paenibactin, a catecholate siderophore produced by *Paenibacillus elgii* B69. *Environ. Microbiol.* **2011**, *13*, 2726–2737. [CrossRef] [PubMed]
67. Javed, Z.; Tripathi, G.D.; Mishra, M.; Dashora, K. Actinomycetes—The microbial machinery for the organic-cycling, plant growth, and sustainable soil health. *Biocatal. Agric. Biotechnol.* **2021**, *31*, 101893. [CrossRef]
68. Huang, K.-C.; Zhao, W.; Li, J.-N.; Mumin, R.; Song, C.-G.; Wang, H.; Sun, Y.-F.; Cui, B.-K. Afforestation-Induced Shifts in Soil Bacterial Diversity and Community Structure in the Saihanba Region. *Microorganisms* **2024**, *12*, 479. [CrossRef]
69. Jiang, Z.M.; Mou, T.; Sun, Y.; Su, J.; Yu, L.Y.; Zhang, Y.Q. Environmental distribution and genomic characteristics of Solirubrobacter, with proposal of two novel species. *Front. Microbiol.* **2023**, *14*, 1267771. [CrossRef]
70. Pozzi, R.; Simone, M.; Mazzetti, C.; Maffioli, S.; Monciardini, P.; Cavaletti, L.; Bamonte, R.; Sosio, M.; Donadio, S. The genus *Actinoallomurus* and some of its metabolites. *J. Antibiot.* **2011**, *64*, 133–139. [CrossRef]

71. Liang, S.-M.; Zheng, F.-L.; Wu, Q.-S. Elucidating the dialogue between arbuscular mycorrhizal fungi and polyamines in plants. *World J. Microbiol. Biotechnol.* **2022**, *38*, 159. [CrossRef] [PubMed]
72. Stenholm, Å.; Backlund, A.; Holmström, S.; Backlund, M.; Hedeland, M.; Fransson, P. Survival and growth of saprotrophic and mycorrhizal fungi in recalcitrant amine, amide and ammonium containing media. *PLoS ONE* **2021**, *16*, e0244910. [CrossRef] [PubMed]
73. Xie, J.; Shi, H.; Du, Z.; Wang, T.; Liu, X.; Chen, S. Comparative genomic and functional analysis reveal conservation of plant growth promoting traits in *Paenibacillus polymyxa* and its closely related species. *Sci. Rep.* **2016**, *6*, 21329. [CrossRef]
74. Eder, S.; Shi, L.; Jensen, K.; Yamane, K.; Hulett, F.M. A Bacillus subtilis secreted phosphodiesterase/alkaline phosphatase is the product of a Pho regulon gene, phoD. *Microbiology* **1996**, *142*, 2041–2047. [CrossRef]
75. Eastman, A.W.; Heinrichs, D.E.; Yuan, Z.-C. Comparative and genetic analysis of the four sequenced *Paenibacillus polymyxa* genomes reveals a diverse metabolism and conservation of genes relevant to plant-growth promotion and competitiveness. *BMC Genom.* **2014**, *15*, 851. [CrossRef] [PubMed]
76. Sekowska, A.; Bertin, P.; Danchin, A. Characterization of polyamine synthesis pathway in *Bacillus subtilis* 168. *Mol. Microbiol.* **1998**, *29*, 851–858. [CrossRef]
77. Xie, J.-B.; Du, Z.; Bai, L.; Tian, C.; Zhang, Y.; Xie, J.-Y.; Wang, T.; Liu, X.; Chen, X.; Cheng, Q. Comparative genomic analysis of N2-fixing and non-N2-fixing *Paenibacillus* spp.: Organization, evolution and expression of the nitrogen fixation genes. *PLoS Genet.* **2014**, *10*, e1004231. [CrossRef]
78. Liu, D.; Perez-Moreno, J.; Zhang, P.; Wang, R.; Chater, C.C.C.; Yu, F. Distinct Compartmentalization of Microbial Community and Potential Metabolic Function in the Fruiting Body of *Tricholoma matsutake*. *J. Fungi* **2021**, *7*, 586. [CrossRef] [PubMed]
79. Dosselaere, F.; Vanderleyden, J. A Metabolic Node in Action: Chorismate-Utilizing Enzymes in Microorganisms. *Crit. Rev. Microbiol.* **2001**, *27*, 75–131. [CrossRef] [PubMed]
80. Carini, P.; Marsden, P.J.; Leff, J.W.; Morgan, E.E.; Strickland, M.S.; Fierer, N. Relic DNA is abundant in soil and obscures estimates of soil microbial diversity. *Nat. Microbiol.* **2016**, *2*, 16242. [CrossRef] [PubMed]

Disclaimer/Publisher's Note: The statements, opinions and data contained in all publications are solely those of the individual author(s) and contributor(s) and not of MDPI and/or the editor(s). MDPI and/or the editor(s) disclaim responsibility for any injury to people or property resulting from any ideas, methods, instructions or products referred to in the content.